Influence of Chitosan and Bentonite Characteristics on Phosphate Removal from Stormwater

Gaurav Verma¹; Jagadeesh Kumar Janga²; Krishna R. Reddy³; and Angelica M. Palomino⁴

¹Dept. of Civil, Materials, and Environmental Engineering, Univ. of Illinois Chicago, Chicago, IL. Email: gverma5@uic.edu

²Dept. of Civil, Materials, and Environmental Engineering, Univ. of Illinois Chicago, Chicago, IL. Email: jreddy3@uic.edu

³Dept. of Civil, Materials, and Environmental Engineering, Univ. of Illinois Chicago, Chicago, IL. Email: kreddy@uic.edu

⁴Dept. of Civil and Environmental Engineering, Univ. of Tennessee Knoxville, Knoxville, TN. Email: apalomin@utk.edu

ABSTRACT

Containment barrier systems, such as vertical slurry walls and low-permeable liners in waste containment systems, are commonly used to prevent groundwater contamination. However, traditional low-permeable clays used in these barriers have limitations in effectively removing various contaminants, including phosphate, which is a contaminant of global concern. The overarching goal of this work is to create a novel chitosan-bentonite composite barrier for improving the performance of containment systems. Chitosan, a material derived by deacetylating chitin, is a promising barrier material due to its ability to adsorb various contaminants. The purpose of this study is to investigate incorporating chitosan into these barriers to enhance their contaminant adsorption capacity. Previous studies were performed on three chitosans with varying degree of deacetylation (DOD) and molecular weights (MW) and one type of bentonite. The current study presents results from batch tests on four additional chitosan materials and a different source of bentonite. These tests assessed their individual phosphate removal capabilities and were compared with earlier findings. The chitosans exhibited varying phosphate removal efficiencies based on DOD, MW, surface area, and source. The highest removal efficiency ranging from 20.9% to 85.6%, at different initial phosphate concentrations, was achieved by one of the chitosan variants. In contrast, bentonite achieved 15.3% to 41.6% removal at different phosphate concentrations. Results suggest a composite material of chitosan and bentonite in engineered barriers could significantly enhance phosphate removal, especially at lower concentrations (0.5 mg/l), compared to a simple bentonite-based barrier.

INTRODUCTION

The increasing global average temperatures and resulting changes in climate patterns have led to a wide range of extreme events, such as frequent flooding, sea level rise, and subsequent saltwater intrusion. These events can have several impacts, including the infiltration of contaminated stormwater into the ground, resulting in groundwater contamination, as well as the intrusion of saltwater into freshwater aquifers. Engineered barriers are employed as a mitigation strategy to address these challenges. For instance, low-permeability liners are installed at the bottom of retention ponds, while vertical slurry walls are constructed around contaminated

groundwater in the subsurface (Sharma and Reddy 2004). These engineered barriers, which employ low-permeability clays like bentonite, effectively reduce the infiltration and passage of contaminated water. However, relying solely on clays has limitations in their ability to effectively adsorb a wide range of contaminants. Therefore, it is crucial to investigate potential alternative materials, to form composites consisting of sustainable low-cost materials with the ability to adsorb a broader range of contaminant types and low permeable clays such as bentonite, for implementation in these engineered barriers.

Chitosan, a biopolymer derived from deacetylating chitin, has immense potential as an effective adsorbent in such composites due to its high adsorption capacity and ease of combining with other materials (Feng et al. 2019). Chitin, the second most abundant natural biopolymer after cellulose, primarily sourced from the exoskeletons of crustacean shells, can also be derived from fungal and plant-based materials (Muzzarelli 1977). The utilization of crustacean shells is particularly desirable as they constitute a significant portion (50-70%) of seafood processing waste and finding beneficial applications for this waste helps in avoiding the environmental costs associated with its disposal (Kumar et al. 2018). Chitosan finds applications in various industries, including cosmetics, medicine, food, and environmental remediation, due to its high adsorption capacity, biodegradability, non-toxic nature, and excellent compatibility with other materials (Synowiecki and Al-Khateeb 2003). Previous research in wastewater treatment has demonstrated that chitosan-based adsorbents are capable of capturing contaminants across a broad concentration spectrum (Bhatnagar and Sillanpää 2009). During the deacetylation process of chitin, free amino groups are generated. The amino (-NH₂) and hydroxyl (-OH) groups in chitosan can act as active adsorption sites for various pollutants such as heavy metals and can form hydrogen bonds with Si-O-Si groups of bentonite leading to stronger interactions between chitosan and bentonite (Feng et al. 2019; Giannakas and Pissanou 2018). Hence, chitosanbentonite composites hold significant potential for effectively functioning as barriers.

Engineered barriers can be a vital system for removing contaminants from stormwater. Phosphate from urban stormwater runoff is a major contributor to nutrient pollution in surface water bodies. Phosphorous contamination in the US has significantly increased since 2004, leading to serious problems related to eutrophication in surface water bodies (USEPA 2013). Often, the source of phosphorous-based nutrients is unknown and assumed to have originated from distant locations (Manuel 2014). Therefore, it is crucial to minimize excessive phosphate exposure to the environment. Consequentially, the current study focuses on evaluating the ability of various types of chitosans and bentonite to adsorb phosphate. Several sets of batch experiments with four different types of chitosans and one type of bentonite were conducted with varying initial phosphate concentrations (0.5-12 mg/l). Results from these batch tests were compared to results from a previous study using three other chitosans and one other bentonite from different sources, for a comprehensive understanding of phosphate removal patterns.

MATERIALS AND METHODS

Materials

Chitosan is derived from the deacetylation process of chitin, a linear mucopolysaccharide primarily found in arthropod exoskeletons and some fungal cell walls. Increasing the duration of the deacetylation process increases the degree of deacetylation (DOD), which corresponds to the removal of acetyl groups. However, prolonged reaction times negatively influence the molecular weight of chitosan, resulting in a decreased number of monomer units in a single polymer chain

(Tsaih and Chen 2003). This reduction in molecular weight implies a lower number of active adsorption sites (Tsaih and Chen 2003). Therefore, the DOD, molecular weight, and source of feedstock are crucial parameters when evaluating the phosphate adsorption capacity of chitosan. Hence, this study utilized four types of chitosan with varying DOD, molecular weight, and source feedstock. The chitosan types selected for this study were from crustacean sources (snow crab, shrimp etc.) and mushrooms. Material properties of the selected chitosans, as provided by the manufacturer as well as fundamental properties measured in the laboratory are presented in Table 1. All varieties of chitosan were purchased from the same commercial source (ChitoLytic, Inc., Ontario, Canada) and were used without modification. The bentonite used in this study was VOLCLAY CP-200, which was acquired from Colloid Environmental Technologies Company (CETCO), USA.

Table 1. Properties of different chitosans and bentonite used in this study

Parameter	Chitosan-1	Chitosan-2	Chitosan-3	Chitosan-4	Bentonite
Symbol	CMMP80	CMHF86.5	CHLP90	MHMP90.1	-
Hygroscopic Moisture (%)	3.6	13.6	8.9	9.5	8.2
Organic content (%)	99.8	98.1	98.9	99	1.2
pH (1:20)	8.4	8.1	8.1	8	9.6
ORP(mV)	229	235	230	233	70.3
EC (mS/cm)	0.18	0.28	0.16	0.22	0.14
Appearance					
Color	White	White	White	White to light yellow	Grey
Form	Powder	Flake	Powder	Powder	Powder
Source*	Crustacean	Crustacean	Crustacean	Mushroom	-
Degree of deacetylation* (%)	> 80	86.5	> 90	90.1	-
Molecular weight* (kDa)	<400	-	-	250-300	
Molecular weight range*	Medium	Very high	Very low	Medium	-
Viscosity* (cps)	-	1200	<30	-	

^{*}Properties as provided by the vendor

Batch Experimental Procedure

The adsorption capacity of chitosans and bentonite were determined using batch experiments. Four different concentrations of phosphate (PO₄³-P) solutions (0.5, 2, 8 and 12 mg/l) were prepared. The preparation of these concentrations involved initially preparing a standard stock solution of 100 mg/l PO₄³-P by dissolving 0.439 g of potassium dihydrogen phosphate (KH₂PO₄) in 1 L of deionized water. Subsequently, the desired phosphate concentrations were obtained by diluting the standard stock solution using the calculated dilution ratios. Chitosans were added to these phosphate solutions and batch tests were performed to evaluate removal efficiencies, and adsorption kinetics through isotherm modeling. Analytical properties, pH, Oxidation Reduction Potential (ORP), Electrical Conductivity (EC), were measured and compared for pre- and post- batch experiment conditions. A brief schematic of methodology followed for batch tests is presented in Figure 1. Further details about the methodology followed for batch tests and analytical property testing were presented in Verma et al. (2023). All batch tests were performed in duplicates to ensure consistency in the obtained results.

Similar batch tests were previously performed on three other chitosans acquired from a different vendor and bentonite acquired from a different source. The properties of the chitosans used in the earlier study, as reported in Verma et al. (2023) are presented in Table 2.

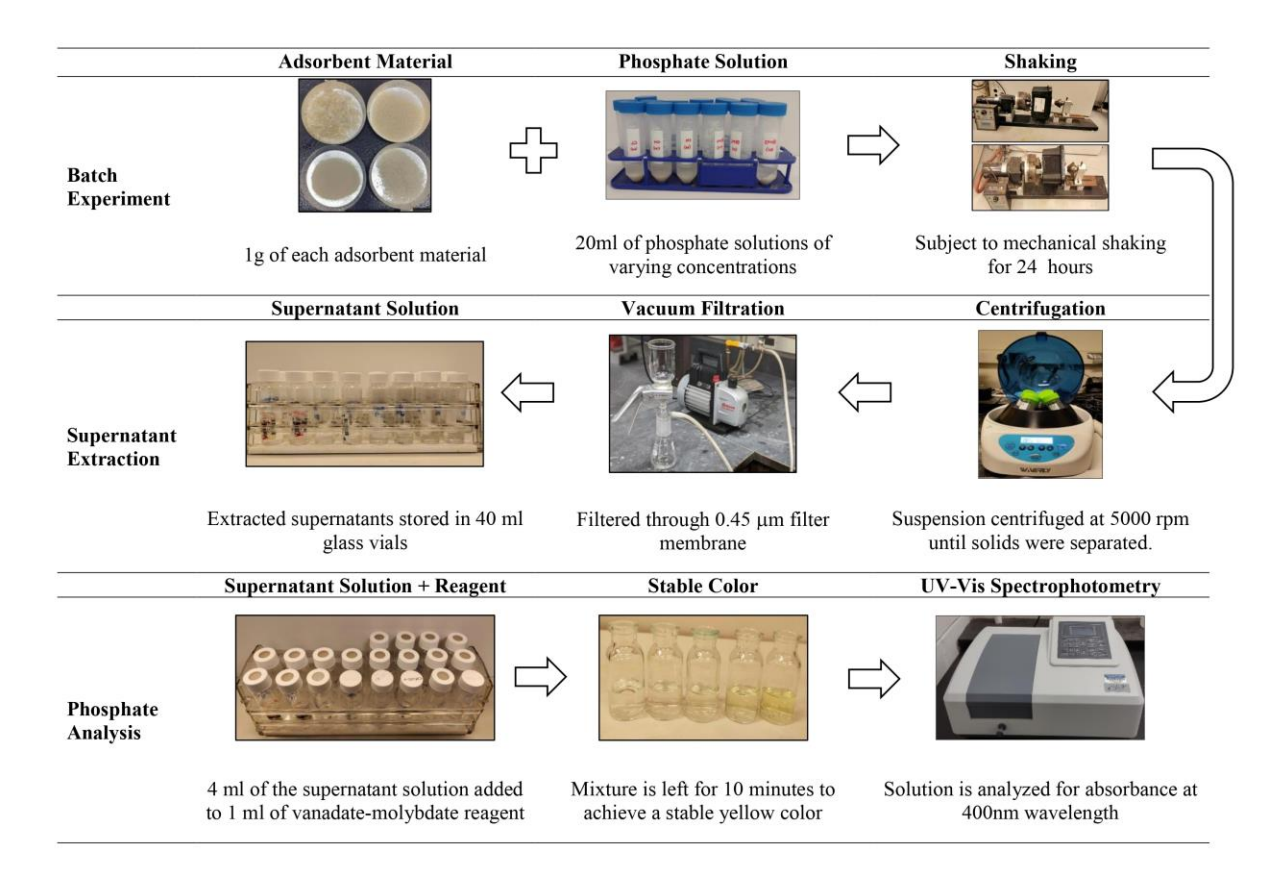


Figure 1. A stepwise illustration of methodology followed for batch experiments

Table 2. Properties of chitosans used in the previous study (Verma et al. 2023), as provided by the vendor

Property	Chitosan-Low	Chitosan-Medium	Chitosan-High
Source	Shrimp shells	Mixed crab and shrimp shells	Shrimp shells
Form	Powder	Crystals	Powder
Molecular weight range	Low	Medium	High
Molecular weight (kDa)	50-190	190-310	310-375
Viscosity (cps)	113	300-494	1218-1232
Degree of deacetylation (%)	76	87-88	76

RESULTS AND DISCUSSION

Filtrate Solution Properties

Figure 2 shows the pH, ORP, and EC of post-filtration supernatant samples from batch tests with the tested materials and initial phosphate solutions. The supernatant properties from the

batch tests for all chitosans were as follows: pH ranged from 7.7 to 8.4, ORP ranged from 213 to 242 mV, and EC ranged from 0.16 to 0.33 mS/cm. There were no clear trends observed for pH and ORP with increasing phosphate concentration, as they remained within a narrow range across all tested concentrations for all the materials. However, a slight increasing trend in EC was observed with increase in phosphate concentrations for all the chitosans. Significant changes were observed between the properties of the post-batch experiment solutions when compared to the initial phosphate solutions at corresponding concentrations. These changes included an increase in pH and EC, indicating higher alkalinity and more number of free ions in the post-batch solutions as well as a decrease in ORP, indicating a less oxidizing environment. The variations in solution properties among different materials primarily stem from inherent material properties, including dissolution reactions within clays, and slight alkaline nature of chitosan, which affects the pH, ORP and EC values of the solution (Verma et al. 2023). Similar solution properties were obtained for all the chitosans used in the previous study (Verma et al. 2023).

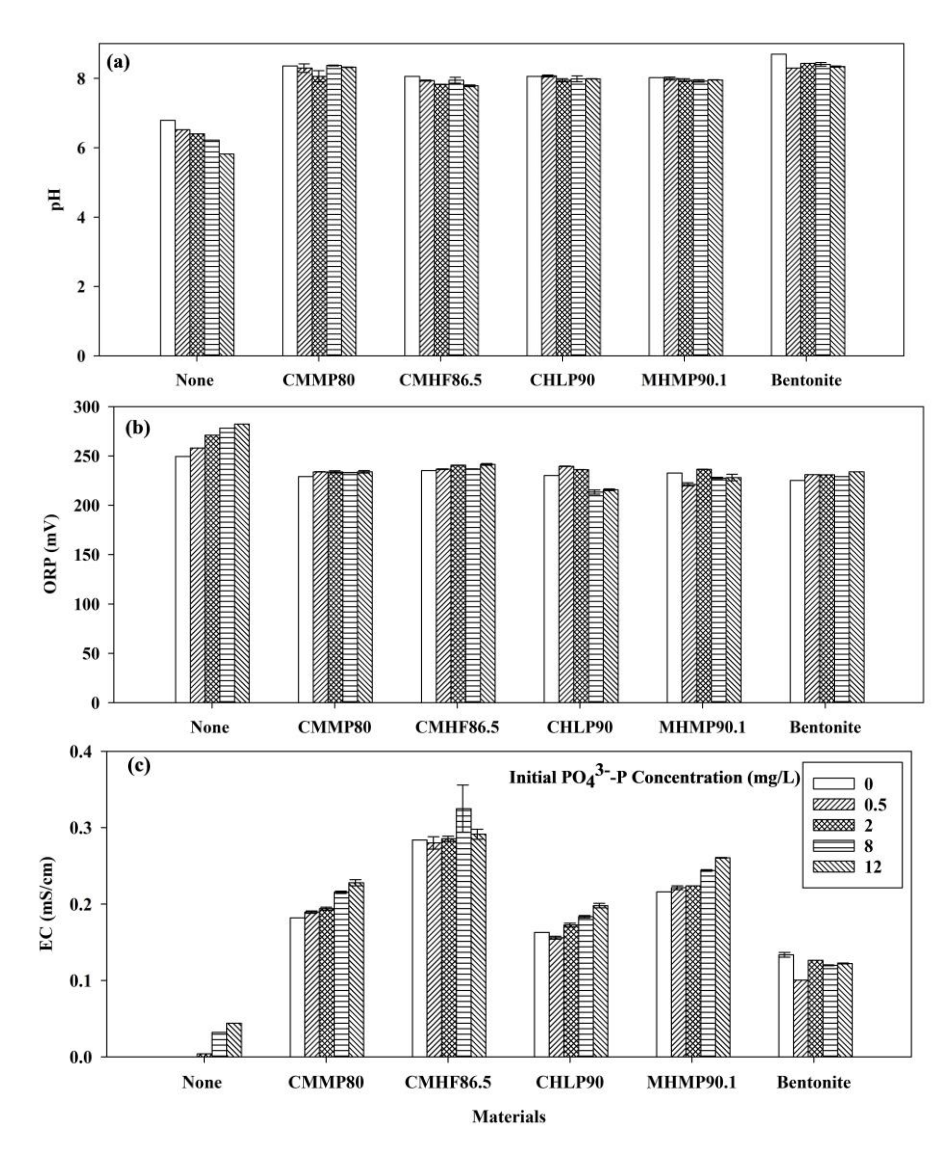


Figure 2. (a) pH, (b) Oxidation-Reduction Potential (ORP), and (c) Electrical Conductivity (EC) of phosphate and supernatant solutions from the adsorbent materials

On comparing the properties of the solutions exposed to chitosan and bentonite, minor differences were observed in pH and ORP. These properties exhibited similar ranges, with pH ranging from 8.3 to 8.5 and ORP ranging from 229 to 234 mV for bentonite. However, a slight decrease in EC (0.1 to 0.13 mS/cm) was noted in the solution exposed to bentonite compared to all chitosan solutions. This slight decrease in EC value is primarily attributed to the inherent EC of the bentonite, meaning that the supernatants from bentonite batch tests had the least number of free ions compared to the tested chitosan materials. However, the bentonite used in the previous study indicated a higher pH and EC, and a lower ORP compared to the values obtained in the current study. Further exploration concerning microstructural and chemical properties of the selected bentonites are needed to understand these differences.

Overall, the results suggest that the initial phosphate concentration had no significant impact on the pH and ORP values of the solutions obtained post-batch experiments conducted with all materials, as they fell within a very narrow range. Based on the similar analytical properties between the tested chitosans when compared to the bentonite used in this study, it can be inferred that making a composite of chitosan and bentonite will likely not disrupt material adsorption due to potential differences in these analytical properties.

Phosphate Removal Efficiency

Figure 3 shows the phosphate removal efficiency of the materials at the selected initial phosphate concentrations. The phosphate removal efficiency results are each presented as the average of two values (duplicate tests). For CMMP80 and CMHF86.5, the phosphate removal efficiencies ranged from 20.9% to 85.6%, and 12.8% to 71.1% respectively. As the initial phosphate concentration increased, the removal efficiency decreased, with the lowest efficiency observed at 12 mg/l for CMMP80. In the case of CMHF86.5 with increasing initial phosphate concentration, the removal efficiency generally decreased, except at 12 mg/l where an increase was observed compared to 8 mg/l. The lowest phosphate removal efficiency was observed at 8 mg/l. Both CMMP80 and CMHF86.5 had a similar DOD range as given in Table 1. One possible reason for the latter showing a lower efficiency in removing phosphate is that the specific surface area (SSA) of a flaky material (CMHF86.5) is generally lower than that of a powdered material (CMMP80) (Ardila et al. 2017), resulting in lower exposure of active adsorption sites.

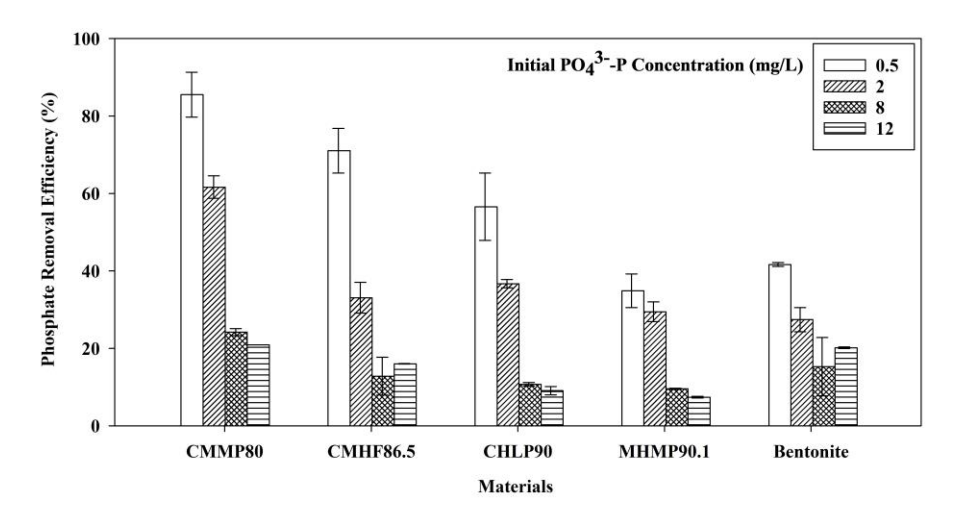


Figure 3. Phosphate removal efficiencies of various adsorbent materials

The batch tests conducted with CHLP90 yielded phosphate removal efficiencies ranging from 9.1% to 56.6%. The lower efficiencies observed for CHLP90 despite having a higher DOD may possibly be due to a significantly lower MW as compared to that of CMMP80 and CMHF86.5 as shown in Table 1 (higher viscosity indicates a higher molecular weight). In the case of CHLP90, a similar trend of decreasing removal efficiencies with increasing initial phosphate concentrations was observed. For MHMP90.1, whose source of feedstock was different from the other three chitosans, the phosphate removal efficiency was consistently lower than all the above chitosans, ranging from 7.4% to 34.9% across the tested initial phosphate concentrations. Similar to CMMP80 and CHLP90, MHMP90 also demonstrated a decreasing trend in phosphate removal efficiency as the initial phosphate concentration increased.

On comparing the phosphate removal efficiency of various chitosans with bentonite, ranging from 15.3% to 41.6%, across different tested phosphate concentrations, a disparity in removal efficiency was observed at the lower concentrations (0.5 and 2 mg/l). However, for higher initial phosphate concentrations (8 and 12 mg/l), the removal efficiency of both chitosan and bentonite were similar. Additionally, all the materials were subjected to batch tests (duplicates) with deionized water (0 mg/l phosphate) to determine if any of the tested materials would release or leach phosphate into the aqueous solution. No detectable release of phosphate was observed for any of the chitosan variants tested. This is because chitosan is primarily composed of organic polymers that do not contain any form of phosphorus. However, a leachable amount of 4.75 mg phosphate per kg of bentonite was observed when tested with deionized water.

When compared to the removal efficiencies observed in the previous study, chitosan-low (19-77 %), chitosan-high (18-55%), chitosan-medium (31-84%), the removal efficiencies obtained for MHMP90.1 and CHLP90 were consistently lower. On the other hand, the phosphate removal efficiencies of CMMP80 and CHMF86.5 were similar to chitosan-medium and chitosan-low, respectively. Removal efficiencies obtained for the bentonite in this study are comparable to that of the efficiencies for the bentonite used in the previous study.

The sorption of phosphate by chitosan is likely mediated through electrostatic attraction between negatively charged PO₄³-P ions and positively charged (protonated) amino groups present on chitosan molecules (Eltaweil et al. 2021). The results obtained from the batch experiments conducted with different chitosan variants showed a descending order of phosphate removal efficiency as follows: chitosan-medium>CMMP80 > chitosan-low>CMHF86.5 > chitosan-high>CHLP90 > MHMP90.1. Surprisingly, no correlation was observed between the DOD and the phosphate removal efficiency, based on the results obtained from the batch experiments. This lack of correlation could be attributed to variations in feedstock source, SSA, and MW among the different chitosans, as these factors will influence the phosphate adsorption capacity significantly (Peniche et al. 2008; Eltaweil et al. 2021). Therefore, it is imperative to conduct further analysis taking into account relevant properties that influence adsorption to gain a better understanding of the variations in phosphate removal exhibited by these materials.

Past research indicates that the removal of phosphate by bentonite is influenced by surface precipitation and adsorption mechanisms. The presence of aluminum and iron oxides in the clay minerals enables ligand exchange, thereby leading to adsorption. Additionally, when phosphate interacts with the free aluminum or iron ions released from the clay minerals, precipitation can occur (Asomaning 2020). The removal efficiencies obtained for some of the chitosans were higher than bentonite at lower concentrations indicating that the use of such composite for engineered barriers can enhance the phosphate removal capability at lower concentrations as

compared to solely bentonite-based barriers. However, consideration should be given to relevant properties of chitosans before preparing such composites.

Isotherm Modeling

Adsorption isotherms show the correlation between the quantities of nutrients (phosphate) adsorbed per unit dry mass of the material and the equilibrium concentration of those nutrients (phosphate) in the solution. In this study, the correlation between phosphate adsorption and equilibrium concentration was established using two models: Langmuir and Freundlich. A detailed description of these models is presented in Verma et al. (2023).

Figure 4 presents the batch sorption test results for the removal of PO₄³-P using chitosan and bentonite. The equilibrium concentration (C) and phosphate removal per unit mass of adsorbent (S) values presented in Figure 4 were used in subsequent modelling with Freundlich and Langmuir isotherms. The Freundlich and Langmuir parameters and corresponding correlation factors obtained for all the tested materials are presented in Table 3. The results indicate that the Langmuir isotherm model best describes the phosphate adsorption for CHLP90, and MHMP90.1, as evidenced by the higher correlation factors. However, for CMHF86.5 and bentonite, the Freundlich isotherm model was found to be the better fit. For CMMP80, both models accurately fit. It can be inferred from the models that, CMMP80 exhibits the highest adsorption capacity for PO₄³-P. Analysis of the isotherms showed that nearly all chitosans (CMMP80, CMHF86.5, CHLP90, and MHMP90.1) reached their maximum adsorption capacity, indicating a limited number of available adsorption sites at higher phosphate concentrations.

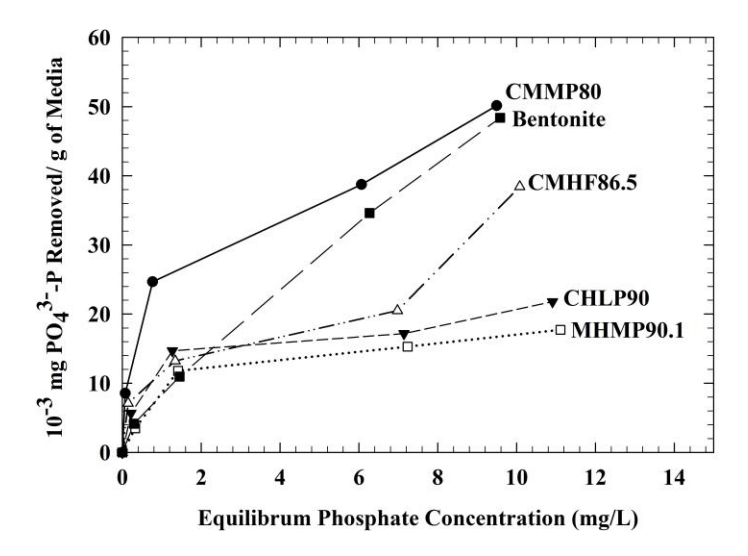


Figure 4. Batch adsorption test results by the selected materials

It is important to note that the maximum sorbed phosphate observed at 12 mg/l was 50.14 mg/kg, 38.41 mg/kg, 21.77 mg/kg, 17.72 mg/kg and 48.39 mg/kg for CMMP80, CMHF86.5, CHLP90, MHMP90.1 and bentonite, respectively. Therefore, it can be deduced that all the tested materials were near their maximum adsorption capacities at 12 mg/l of initial phosphate concentration, with the exception of CMHF86.5 and bentonite. In the case of CMHF86.5, the maximum adsorption capacity estimated using the Langmuir isotherm model was lower than what was observed in the isotherm graph. Conversely, for bentonite, the maximum adsorption

capacity was higher compared to all the chitosan variants, despite exhibiting lower phosphate removal efficiency at each tested concentration when compared to the three chitosan variants (CMMP80, CMHF86.5, CHLP90) (Figure 3). This discrepancy can be attributed to the inadequate fit of the Langmuir isotherm model for CMHF86.5 and bentonite. However, comparison of Freundlich parameter, K, shows a different scenario where bentonite had capacity (represented by K) similar to that of CHLP90 and MHMP90.1 which agrees with the removal efficiencies obtained. The differences in the isotherm parameters between the materials used in the past study (Verma et al. 2023) are consistent with that of the differences observed in removal efficiencies. For the purpose of brevity, these differences are not elaborated on in this paper.

Table 3. Freundlich and Langmuir isotherm model parameters for all the liner materials.

Materials	Freundlich ($S = KC^N$)			Langmuir $(S = \frac{\alpha\beta c}{1+\alpha c})$		
	K	N	R^2	α	β	R^2
CMMP80	22.88	0.35	0.98	1.29	50.51	0.97
CMHF86.5	13.12	0.35	0.91	0.50	36.76	0.76
CHLP90	10.44	0.31	0.90	1.18	21.98	0.97
MHMP90.1	6.98	0.43	0.88	0.76	19.31	0.99
Bentonite	9.39	0.71	0.99	0.13	81.30	0.85

Note: $K(mg^{l-N}l^N/kg)$, N – Freundlich isotherm constants, $\alpha l/mg$) – adsorption constant related to binding energy, $\beta (mg/kg)$ – maximum contaminant adsorption capacity

CONCLUSIONS

The goal of this study is to assess the phosphate adsorption capacity of four chitosan variants with varying degrees of deacetylation, source, and molecular weight: CMMP80, CMHF86.5, CHLP90 and MHMP90.1, and bentonite. The results obtained in this study were also compared to the results obtained from a previous study conducted using three other chitosans with different properties and another bentonite from a different source. Batch experiments were conducted individually for each material at different initial phosphate concentrations. Measurements of pH, ORP, and EC indicated no significant differences among all the tested materials. The findings of the batch experiments on materials tested in the current study revealed that MHMP90.1 exhibited the lowest phosphate removal efficiency, while CMMP80 demonstrated the highest efficiency, ranging from 20.9% to 85.6% with initial phosphate concentration ranging between 0.5-12 mg/l. Various properties of chitosan such as degree of deacetylation, molecular weight, surface area, and source of feedstock can be some of the controlling parameters responsible for the differences in removal efficiencies observed. The removal efficiency obtained for bentonite was 15.3 to 41.6% at different tested phosphate concentrations. The Langmuir isotherm model was found to best describe the phosphate adsorption for CMMP80, CHLP90, and MHMP90.1, while the Freundlich isotherm model was more suitable for CMMP80, CMHF86.5, and bentonite. Overall, based on the removal efficiencies and adsorption capacities obtained from the isotherms it can be concluded that the chitosan, with favorable properties, can be efficient in adsorbing phosphate at lower concentrations. However, further research is warranted to explore its effectiveness when combined with other materials like bentonite. Additionally, future research should encompass a broader range of contaminants and different chitosan composites for a comprehensive assessment of the utility of chitosan in engineered barriers.

ACKNOWLEDGEMENT

This research is a part of comprehensive project titled "Development of Novel Chitosan-Biochar-Bentonite Composite Barrier Resilient to Changing Climate: Synthesis, Characterization, and Containment Mechanisms" funded by the National Science Foundation (CMMI# 2225303), which is gratefully acknowledged. Any opinions, findings, conclusions, and recommendations expressed in this material are those of the authors and do not necessarily reflect the views of the NSF.

REFERENCES

- Ardila, N., Daigle, F., Heuzey, M. C., and Ajji, A. (2017). Antibacterial activity of neat chitosan powder and flakes. *Molecules*, 22(1), 100.
- Asomaning, S. K. (2020). Processes and factors affecting phosphorus sorption in soils. In *Sorption in 2020s*, 45: 1-16.
- Bhatnagar, A., and Sillanpää, M. (2009). Applications of chitin-and chitosan-derivatives for the detoxification of water and wastewater—a short review. *Advances in Colloid and Interface Science*, 152(1-2), 26-38.
- Eltaweil, A. S., Omer, A. M., El-Aqapa, H. G., and Gaber, N. M. (2021). Chitosan based adsorbents for the removal of phosphate and nitrate: A critical review. *Carbohydrate Polymers*, 274, 118671.
- Feng, G., Ma, J., Zhang, X., Zhang, Q., Xiao, Y., Ma, Q., and Wang, S. (2019). Magnetic natural composite Fe3O4-chitosan@ bentonite for removal of heavy metals from acid mine drainage. *Journal of Colloid and Interface Science*, 538, 132-141.
- Giannakas, A., and Pissanou, M. (2018). Chitosan/bentonite nanocomposites for wastewater treatment: a review. *SF J Nanochem Nanotechnol*. 2018; 1 (1), 1010.
- Kumar, A., Kumar, D., George, N., Sharma, P., and Gupta, N. (2018). A process for complete biodegradation of shrimp waste by a novel marine isolate Paenibacillus sp. AD with simultaneous production of chitinase and chitin oligosaccharides. *International Journal of Biological Macromolecules*, 109, 263-272.
- Manuel, J. (2014). Nutrient pollution: A persistent threat to waterways. *Environ. Health Perspect*, 122, A304–A309.
- Muzzarelli, R. A. A. (1977). *Chitin*. Pergamon Press, New York, NY.
- Peniche, C., Argüelles-Monal, W., and Goycoolea, F. M. (2008). Chitin and chitosan: major sources, properties and applications. In *Monomers, Polymers and Composites from Renewable Resources* (pp. 517-542). Elsevier.
- Sharma, H. D., and Reddy, K. R. (2004). *Geoenvironmental Engineering: Site Remediation, Waste Containment, and Emerging Waste Management Technologies*. John Wiley, Hoboken, NJ.
- Synowiecki, J., and Al-Khateeb, N. A. (2003). Production, properties, and some new applications of chitin and its derivatives. *Critical Reviews in Food Science and Nutrition*, 43(2), 145-171.
- Tsaih, M. L., and Chen, R. H. (2003). The effect of reaction time and temperature during heterogenous alkali deacetylation on degree of deacetylation and molecular weight of resulting chitosan. *Journal of Applied Polymer Science*, 88(13), 2917-2923.

USEPA (United States Environmental Protection Agency). (2013). National rivers and streams assessment 2008–2009: A collaborative survey (Draft). USEPA, Washington, DC. https://www.epa.gov/national-aquatic-resource-surveys/nrsa (May 21, 2023).

Verma, G., Janga, J. K., Reddy, K. R., and Palomino, A. M. (2023). Phosphate removal from synthetic stormwater using chitosan and clay. *Journal of Hazardous, Toxic, and Radioactive Waste*, ASCE.